Fibers and Polymers 2011, Vol.12, No.1, 65-72 DOI 10.1007/s12221-011-0065-9

Preparation and Characterization of PVA/PU Blend Nanofiber Mats by Dual-jet Electrospinning

Mingbo Gu[1], Kaitao Wang[1], Wenli Li[1], Chuanxiang Qin[1]*, Jian-Jun Wang[1], and Lixing Dai[1,2]**

[1]*College of Chemistry, Chemical Engineering and Materials Science, Soochow University, Suzhou, China*
[2]*National Engineering Laboratory for Modern Silk, Soochow University, Suzhou, China*
(Received July 21, 2010; Revised October 13, 2010; Accepted October 24, 2010)

Abstract: A series of blend nanofiber mats comprising poly(vinyl alcohol) (PVA) and polyurethane (PU) were prepared by dual-jet electrospinning in various parameters. Orthogonal experimental design was used to investigate how those parameters affected on fiber diameters and fiber diameter distribution. Altogether three parameters having three levels each were chosen for this study. The chosen parameters were tip-to-collector distance (TCD), voltage and tip-to-tip distance (TTD). Fiber diameters, thermal properties, mechanical properties and hydrophilicity of the blend nanofiber mats were examined by scanning electron microscopy (SEM), thermogravimetric analysis (TGA), tensile test, contact angle and water absorption test, respectively. The results showed that the optimum conditions for PVA/PU blend nanofiber mats fabricated by dual-jet electrospinning were TCD of 20 cm, voltage of 18 kV and TTD of 4 cm. Besides, the thermal stability of PVA/PU blend nanofiber mats had been improved compared with pure nanofibers. Furthermore, the elongation and tensile strength of the blend nanofiber mats were significantly increased compared with pure PVA and pure PU, respectively. And the blend nanofiber mats exhibited well hydrophilicity.

Keywords: Nanofiber, Dual-jet electrospinning, Poly(vinyl alcohol), Polyurethane

Introduction

In past decades, much attention has been paid to electrospinning which can produce fibers with diameters ranging from several microns down to 100 nm or less under a high-voltage electrostatic field [1], because of the unique properties of electrospun nanofibers, such as large specific surface area to volume ratio, small pore size and superior performance of mechanical properties [2]. Many kinds of polymers, such as poly(vinyl alcohol) (PVA) [3], poly(ethylene oxide) [4], polyurethane (PU) [5], poly(trimethylene carbonate) [6] and cellulose acetate [7] can be formed nanofibers by use of electrospinning. A number of nanofibers produced by electrospinning have a broad range of applications such as tissue engineering [8], sensor [9], filter [10], and so on. Among these electrospinning polymer nanofibers, PVA is a kind of water-soluble polyhydroxy polymer. And it has an inherent fiber- and film-forming ability, excellent chemical resistance and complete biodegradability which lead to broad practical applications ranging in biomedical, cosmetic, food, pharmaceutical, and packaging industries [11-13].

PVA nanofibers have been successfully electrospun from aqueous PVA solution and maintain fibrous structure in water environment after heat treatment [14]. Researchers have studied the PVA blend fibers with other polymers produced by electrospinning, such as chitosan [15,16], polypropylene [17], and so on. However, there are few reports describing PVA/PU blend nanofibers produced by electrospinning. PU is a versatile polymer with unique properties that are used in a broad range of applications due to its excellent physical properties and relatively good biocompatibility [18]. Researchers [19-22] have studied electrospun PU nanofibers which could be used as wound dressing, shape memory material, and so on. PU blends with poly(vinyl chloride), cellulose acetate, polycarbonate and silver nanoparticles have been reported [23-25,5]. The performance of PU may be improved by blending it with appropriate polymers in view of the fact that polymer blends have provided an efficient way to fulfill new requirements for material properties. Therefore, authors try to produce the PVA and PU blend nanofibers with high strength, flexibility and hydrophilicity.

Conventionally, electrospinning is reported using single-jet, but the blend nanofiber mats of PVA and PU have not been reported because it is difficult to find a good solvent for preparing the blend solution of PVA and PU which can be electrospun using single-jet. So, authors try to use a dual-jet electrospinning method to prepare the PVA/PU blend nanofiber mats. This approach can be used to fabricate blend nanofiber mats from two different polymers which can not be dissolved in the same solvent or can not disperse into each other very well. Furthermore, dual-jet, even multi-jet electrospinning will provide a possibility of industrialization of electrospinning.

In this paper, a series of PVA/PU blend nanofiber mats have been prepared by dual-jet electrospinning. The optimum electrospinning conditions have been determined by the method of orthogonal experiment design, such as tip-to-collector distance (TCD), voltage and tip-to-tip distance (TTD). After determining the optimum conditions of dual-jet electrospinning PVA/PU blend nanofiber mats, the

*Corresponding author: qinchuanxiang@suda.edu.cn
**Corresponding author: dailixing@suda.edu.cn

thermal properties, mechanical and hydrophilic properties of PVA/PU blend nanofiber mats have been investigated.

Experimental

Materials

PVA was purchased from Sinopharm Chemical Reagent Co., Ltd. (DP=1750±50, deacetylation degree >98 %). PU was offered by Taicang Jinxiang Spandex Fiber Co., Ltd. ($\overline{M}_w \approx 200000$, T_g=−50~−38 °C). Other chemical reagents were purchased commercially and used without further purifying.

Orthogonal Experiment Design

Orthogonal experiment design was formulated in a way that minimizes the number of experiments, but they still contain an extensive set of variables that affects the performance [26]. Each experiment was conducted with the predefined combination of different levels of variables, and the performance of each individual variable could be calculated separately providing it was independent of the other variables. Table 1 shows three parameters with three levels each in this study. TCD had three levels (12, 16, and 20 cm), as well as voltage (12, 15, and 18 kV) and TTD (3, 4, and 5 cm).

Table 1. Parameters and levels for orthogonal experiment

Variable	Level		
	1	2	3
A, TCD (cm)	12	16	20
B, voltage (kV)	12	15	18
C, TTD (cm)	3	4	5

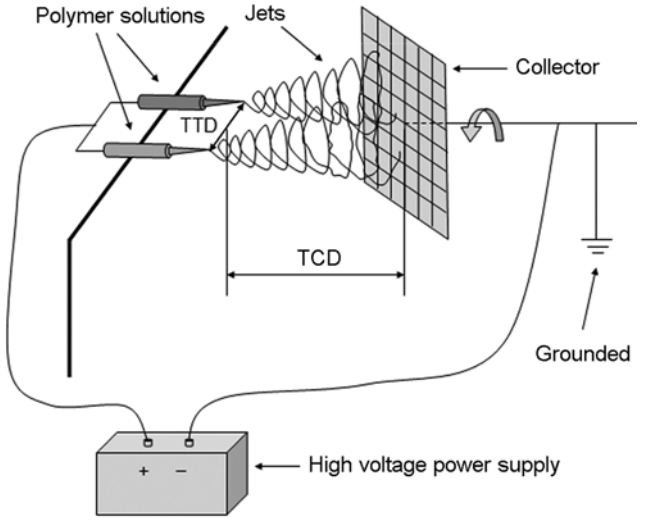

Figure 1. Schematic of electrospinning process.

Preparation of PVA/PU Blend Nanofiber Mats by Dual-jet Electrospinning

Figure 1 shows the schematic of the electrospinning process. A variable high-voltage power supply was used to produce voltages ranging from 0 to 50 kV. PVA/H_2O (7 wt%) and PU/DMF (7 wt%) solutions were poured into different syringes (5 m*l*) attached to a capillary tip with a 0.5 mm diameter. The positive electrode of the high voltage power supply was attached to a copper wire inserted into the polymer solutions. The negative electrode was attached to the grounded collector, which was covered by a piece of aluminum foil and rotated at 140 rpm. The TCD, voltage and TTD were set according to the experimental requirements. The PVA/PU blend nanofiber mats were collected on the surface of aluminum foil and dried at 80 °C in vacuum for 24 h.

Determination of Properties of Solutions and Composition of PVA/PU Blend

Conductivity and viscosity of PVA/H_2O (7 wt%) and PU/DMF (7 wt%) solutions were measured by an electric conductivity meter (DDS-11A, Shanghai Shengci Instrument Co., Ltd) and a rotational viscosimeter (NXS-11A, Chengdu Instrument Factory), respectively. PVA solution had a much higher conductivity (50.0 ms/m) than PU solution (0.3 ms/m), while the viscosity of PU solution (1.7 Pa·s) was much higher than that of PVA (0.4 Pa·s).

Composition of PVA and PU in blend nanofiber mats was determined by immersing the dried blend nanofiber mats into deionized water at 60 °C to remove the PVA component. The immersion time was 72 h. Then, the wet nanofiber mats were dried at 80 °C in vacuum for 24 h. The content of PVA was calculated based on the complete weight loss of PVA during immersion. The weight ratio of PVA/PU in the blend nanofiber mats was about 2/3 and the throughput of PVA and PU nanofibers was 0.9 and 1.3 mg/min·jet, respectively.

Characterization

SEM images of the PVA/PU blend nanofiber mats were observed with scanning electron microscopy (SEM, S-4700, Hitachi Co., Tokyo, Japan). Each SEM sample was divided into three regions (marked I, II, and III) from left to right. And 17 measurements were conducted from each of the regions, so that altogether 50 separate measurements were conducted from each experiment. The average diameter and its standard deviation (SD) were calculated using Microsoft Excel.

Thermogravimetric analysis (TGA) was performed in a Perkin-Elmer TGA-7 analyser (Perkins-Elmer Co., America) under N_2 atmosphere, at a heating rate of 5 °C/min. The crystallinity of PVA nanofiber mats were measured with an X'Pert-Pro MPD diffractometer (XRD, PANalytical, Holland).

Mechanical properties of the PVA/PU blend nanofiber mats were determined with an Instron 1122 automated materials testing system (Instron Ltd., Buckinghamshire, England) at room temperature. The tests were performed at a

constant crosshead speed of 20 mm/min. The size of the samples was 80 mm in length, 10 mm in width, and the gauge length was 50 mm.

The PVA or PVA/PU blend nanofiber mats were heat-treated in a vacuum oven at 155 °C for 5 min to make the PVA component insoluble in water before water contact angles and absorption tests. Fourier transform infrared spectroscopy (FT-IR, Nicolet 5700, America) was used to identify whether the heat treatment had an effect on the chemical structure of PVA, PU and PVA/PU blend nanofiber mats. Contact angles of electrospun nanofiber mats were measured by the sessile water drop method using a contact angle measurement system (DSA 100, Kruss GmbH, Germany) at room temperature. Water droplets (about 5 μl) were dropped carefully on the sample surface. The average contact angle was obtained by measuring the same sample at 5 different sites. Water absorption was measured by immersing the electrospun nanofiber mats in deionized water at 25 °C for 24 h. Then the electrospun nanofiber mats were taken out, and the wet weight of the mats was determined immediately by wiping off the surface water with tissue paper. Each water absorption report was the average value of five measurements. The water absorption was then calculated by the following equation, $W(\%)=(W_w-W_d)/W_w\times 100$, where W_d and W_w were the weights of dry and corresponding water-absorbed electrospun nanofiber mats [27], respectively.

Results and Discussion

Determination of Electrospinning Conditions

Optimum conditions for PVA or PU nanofibers using single-jet electrospinning have been successfully produced [28,29]. However, no reports discussing the conditions of PVA/PU blend nanofibers which produced by dual-jet electrospinning could be found by authors. The optimum electrospinning conditions could be determined by the average diameter and diameter distribution of nanofibers, where diameter distribution could be characterized by SD of fiber diameter [30]. In this paper, with the method of orthogonal experiment design, the influences of three parameters (TCD, voltage and TTD) on the average diameter and its SD of PVA/PU blend nanofibers produced by dual-jet electrospinning were studied, and then the optimum electrospinning conditions were obtained.

Table 2 lists the results of orthogonal experiment and extreme difference analysis. Figure 2 and Figure 3 presents the mean effect of the parameters on fiber diameter and the SD of the fiber diameter, respectively. In Table 2, R was the extreme difference value of the three levels, and importance of the parameter was determined by R, the parameter with the largest R being the most important. The influence on the fiber diameter decreased in the order: A>C>B according to the $R_{Ave.}$ values. So the main parameter affecting the fiber diameter was TCD, while the effect of voltage and TTD was relatively minor. The influence on the SD of fiber diameter decreased in the order: C>A>B according to the R_{SD} values. So the main parameter affecting the fiber diameter distribution seemed to be TTD.

Voltage also could be considered an important essential parameter in electrospinning, since it initiated the jetting and caused instabilities, which stretch the jets [31]. Decreasing fiber diameter due to the higher voltage could be easily

Table 2. Analysis of $L_9(3)^3$ experiment results

No.*	A, TCD (cm)	B, voltage (kV)	C, TTD (cm)	Fiber diameter (nm)				
				I	II	III	Ave.	SD
1	1	1	1	188	197	201	195	6.7
2	1	2	2	183	185	182	183	1.5
3	1	3	3	194	190	191	192	2.1
4	2	1	2	181	179	181	180	1.2
5	2	2	3	190	192	186	189	3.1
6	2	3	1	188	183	180	184	4.0
7	3	1	3	183	181	180	181	1.5
8	3	2	1	169	167	172	169	2.5
9	3	3	2	162	162	161	162	0.6
$K_{1,Ave.}$	570	556	548	-	-	-	-	-
$K_{2,Ave.}$	553	541	525	-	-	-	-	-
$K_{3,Ave.}$	512	538	562	-	-	-	-	-
$R_{Ave.}$	19.3	6.0	12.3	-	-	-	-	-
$K_{1,SD}$	10.3	9.4	13.2	-	-	-	-	-
$K_{2,SD}$	8.3	7.1	3.3	-	-	-	-	-
$K_{3,SD}$	4.6	6.7	6.7	-	-	-	-	-
R_{SD}	1.9	0.9	3.3	-	-	-	-	-

*K_n = Sum (three results of level n), where n=1, 2, and 3, respectively, R=1/3[(Max number of K_1, K_2, and K_3) − (Min number of K_1, K_2, and K_3)].

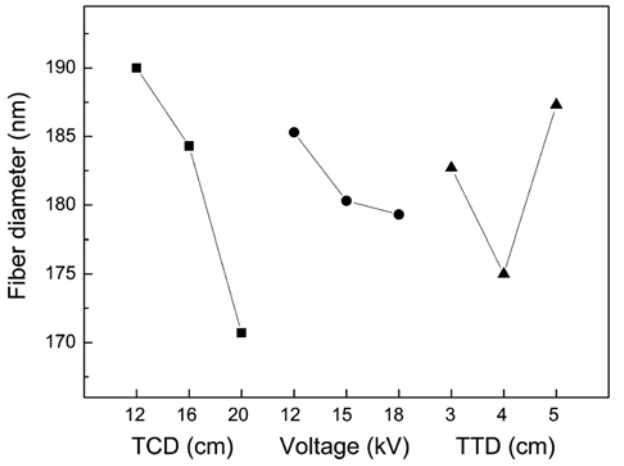

Figure 2. Mean effects of the parameters on the fiber diameter.

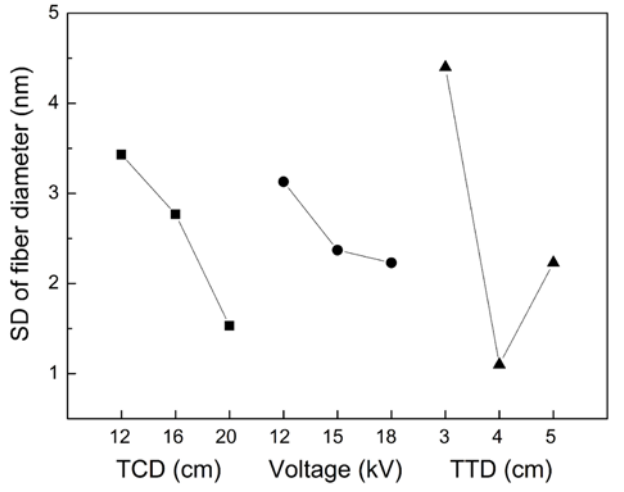

Figure 3. Mean effects of the parameters on the SD of fiber diameter.

explained, since the higher voltage induced higher electrostatic forces on the jet [32], and the higher repulsive forces leaded to the thinner fiber [33]. The voltage determined the average strength of the electric field together with the TCD and TTD. Lager TCD could give more time for the charged jet to split and elongate more times, which lead to thinner fibers [34,35]. The TTD affected the repulsive action between the two jets [36,37]. Figure 4 shows SEM images of pure PVA, PU and PVA/PU blend nanofiber mats, where the pure PVA and PU nanofibers were electrospun at TCD of 20 cm and voltage of 18 kV by single-jet. The diameter of PU nanofibers was much thicker than that of PVA. Consequently, combining the results showed in Table 2 and Figure 3, Figure 4, the optimum conditions of electrospinning PVA/PU blend nanofiber mats by dual-jet were TCD of 20 cm, voltage of 18 kV and TTD of 4 cm in this study.

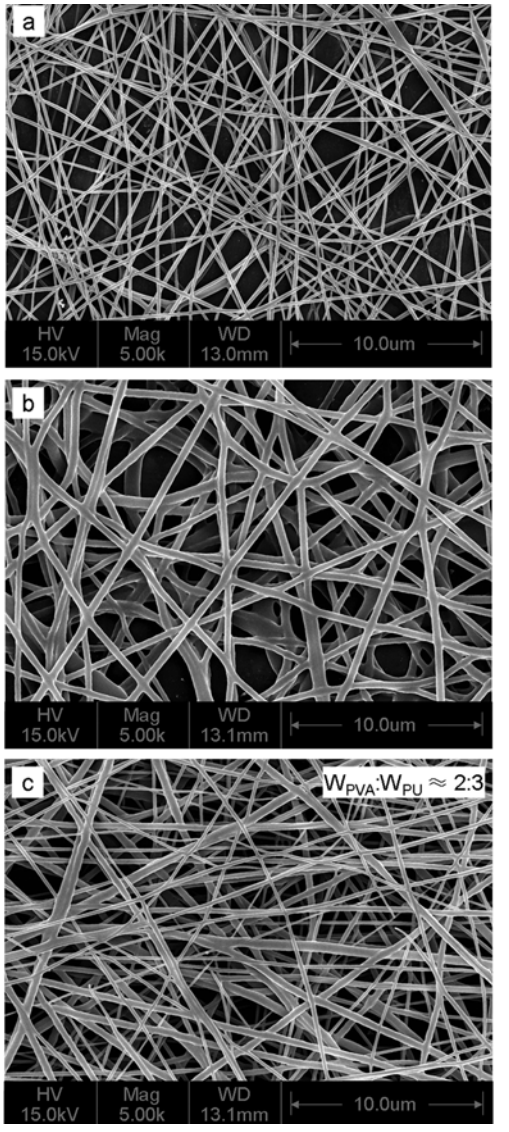

Figure 4. SEM images of electrospun nanofiber mats (a) PVA, (b) PU, and (c) PVA/PU.

Thermal Properties

Figure 5 shows TGA and DTG curves of electrospun nanofiber mats. It can be seen that PVA nanofiber mats began to decompose below 200 °C, and the decomposition rate reached the maximum at about 300 °C. PU nanofiber mats began to decompose at about 250 °C, and there were two different stages of decomposition in DTG curve which were not perceptible in TGA curve, showed the close relation and mutual influence between degradation of hard and soft segments [38]. The maximum decomposition rates of hard and soft segments were observed at about 342 and 420 °C, respectively.

As can be seen from TGA curve, PVA/PU blend nanofiber

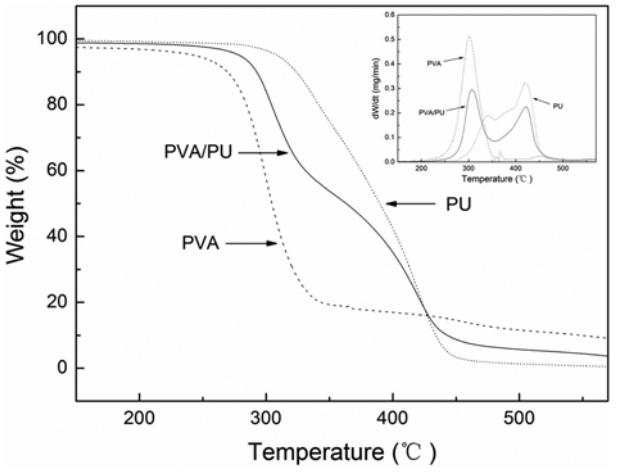

Figure 5. TGA and DTG (upper right) curves of electrospun nanofiber mats.

mats began to decompose near 200 °C, and the thermal decomposition process was composed of two stages, that represented PVA and PU thermal decomposition, respectively. Similarly, DTG curve of PVA/PU blend nanofiber mats showed two peaks obviously at about 307 and 422 °C, which were corresponding to the maximum decomposition rates of pure PVA and PU nanofiber mats, respectively. It illustrated that the two nanofibers had not formed co-crystal structure, PVA crystalline region and PU crystalline region co-existed in blend nanofibers [39]. However, the starting decomposition temperature of PVA/PU blend nanofiber mats was higher than that of pure PVA nanofiber mats and the positions of two decomposition rate peaks slightly shifted to higher temperature. It was suggested that thermal stability of PVA/PU blend nanofiber mats was improved due to high thermal stability of PU.

Mechanical Properties

Table 3 shows the mechanical properties of electrospun nanofiber mats, where each datum is obtained by averaging the results of ten test samples. When the PVA/PU blend nanofiber mats were prepared by dual-jet electrospinning, the tensile strengths and elongation at break were influenced by the structure and properties of each polymer in the blend nanofibers [23].

As can be seen from Table 3, the tensile strength of pure PVA nanofiber mats (13.5 MPa) was higher than that of pure PU nanofiber mats (7.2 MPa), while elongation at break of PVA (51.4 %) was lower than that of PU (98.3 %). As mentioned above, the weight ratio of PVA/PU in the blend nanofiber mats was about 2/3. The tensile strength and elongation at break of PVA/PU blend nanofiber mats were 10.8 MPa and 79.7 %, respectively. It was obvious that these results were strongly dependant on the weight ratio of PVA/PU in the blend nanofiber mats, and the modulus showed the similar results. The PVA/PU blend nanofiber mats were more flexible than pure PVA nanofibers and stronger than pure PU nanofibers. There was a complementary effect on mechanical properties between PVA and PU component in the blend nanofiber mats.

Table 3. Mechanical properties of electrospun nanofiber mats

Samples	Tensile strength (MPa)	Elongation at break (%)	Modulus (MPa)
PVA/PU	10.8	79.7	32.5
PVA	13.5	51.4	45.7
PU	7.2	98.3	21.4

Structure Changes After Heat Treatment

It was reported that simple heat treatment of the electrospun PVA nanofibers could preserve the web structure of the PVA nanofibers in water [14]. In this study, the PVA nanofiber and PVA/PU blend nanofiber mats were heat-treated in a vacuum oven at 155 °C for 5 min to make the PVA component insoluble in water. Figure 6 shows the XRD patterns of electrospun PVA nanofiber mats with or without heat treatment. The XRD patterns revealed that PVA was characterized by semicrystalline structure. There was an intense peak appearing at 2θ=19.6 ° either heat-treated or no-treated of PVA nanofibers mats. The crystalline of PVA resulted from the strong intermolecular interaction between PVA chains through intermolecular hydrogen bonding, and the intensity of the diffraction peak and also the size of the crystals in PVA were determined by the number of PVA chains packed together [40]. It was obvious that the intensity of the PVA diffraction peak was increased after the heat treatment, even some weak peaks of curve of the no-treated PVA nanofiber mats were observed distinctly (2θ=11.3 ° and 22.7 °). The change of the intensity of all these peaks

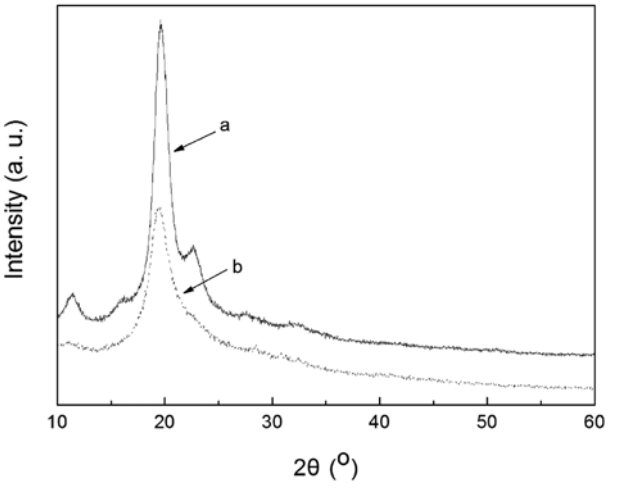

Figure 6. XRD patterns of electrospun PVA nanofiber mats after (a) heat treated and (b) untreated.

demonstrated that heat treatment could improve the crystallinity of PVA and then avoid PVA dissolved in water.

Besides, in an effort to know whether the heat treatment had an effect on the chemical structure of PVA, PU or PVA/PU blend nanofiber mats, FT-IR spectra before and after heat-treatment was compared. As shown in Figure 7(a), it was found that 2940 and 1426 cm^{-1} bands, characteristic of CH_2, and 1092 cm^{-1} band, characteristic of C-O, remained unchanged after heat treatment, while crystalline-sensitive peak at 1140 cm^{-1} showed a definite increase, indicating that the crystallinity of PVA nanofiber mats increased after heat treatment [41]. In this case, it was consistent with the results of XRD analysis as stated above. Peak at 919 cm^{-1} slightly weakened due to the decrease of the amorphous region [42]. Similarly, contrast two FT-IR spectra of PU nanofiber mats shown in Figure 7(b), the characteristic absorption peaks were appeared in both spectra and not changed obviously. The characteristic peaks exhibited at 3331, 2940, 1730, 1600, 1530 cm^{-1} were corresponded to the N-H, CH_2, C=O, C=C (benzene ring), C-N-H, respectively [43,44]. As can be seen from thermal analysis, the thermal degradation of PU nanofibers was very little at the heat treatment temperature 155 °C as shown in Figure 5. And there was no peak at 2340 cm^{-1}, which corresponded to free isocyanate, the degradation product of PU [45]. FT-IR spectra of PVA/PU blend nanofiber mats (Figure 7(c)) showed the same and plus change trend as discussed above. Therefore, it was suggested that heat treatment had no effect on the chemical structure of PVA, PU or PVA/PU blend nanofiber mats.

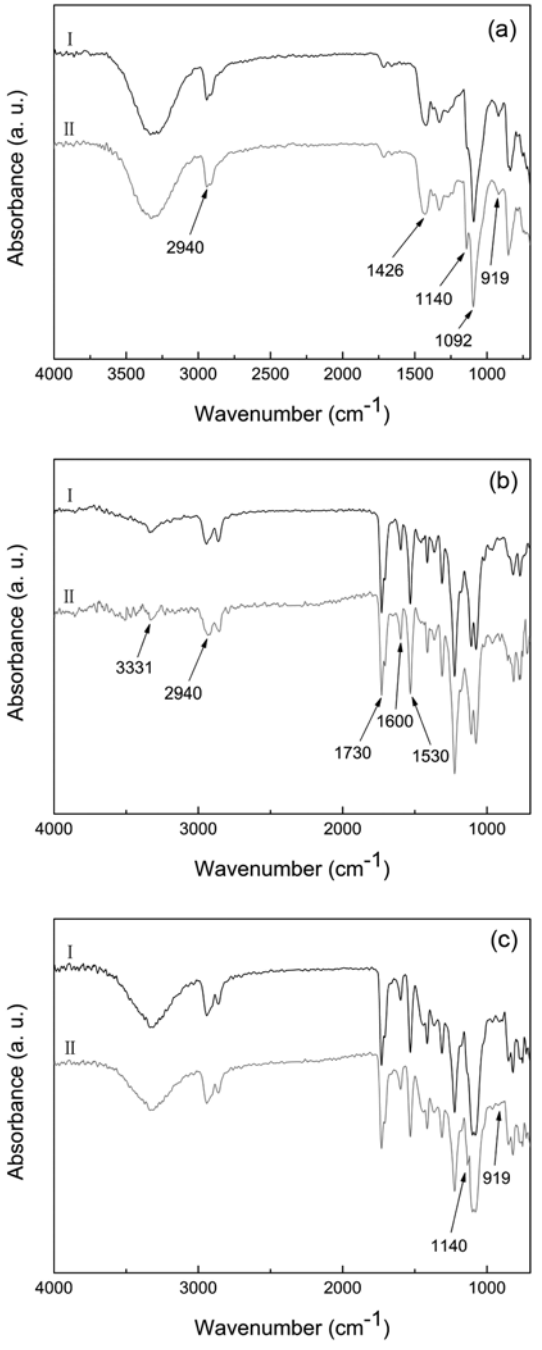

Figure 7. FT-IR spectrum of (a) PVA, (b) PU, and (c) PVA/PU blend nanofiber mats after untreated (Curve I) and heat treated (Curve II).

Hydrophilicity

It was well known that PVA was a good hydrophilic polymer, while PU was a hydrophobic polymer. So it was necessary to check out that whether the incorporation of PU nanofibers decreased the hydrophilicity of the PVA/PU blend nanofiber mats. The hydrophilicity could be characterized by contact angle [46] and water absorption [27].

Table 4 lists the water contact angles of PVA, PU and PVA/PU blend nanofiber mats. When the contact angle was less than 90 °, the mats were hydrophilic and the smaller contact angle, the better hydrophilicity. Conversely, when the contact angle was greater than 90 °, the mats were hydrophobic. Figure 8 illustrates the images of 5 μl water droplets residing on the surface of electrospun nanofiber mats. The water contact angles of the PVA and PU nanofiber mats were 42.5 ° (Figure 8(b)) and 115.0 ° (Figure 8(c)), respectively. And the water droplet had a much spreading on the surface of PVA nanofiber mats, while it had a small contact area with the surface of PU nanofiber mats. Comparing with Figure 8(c), the water droplet in Figure 8(a) shows a smaller contact angle (52.0 °) and larger contact area with the surface of PVA/PU blend nanofiber mats, exhibiting well hydrophilicity. So the incorporation of PU nanofibers had only a little impact on the hydrophilicity of the PVA/PU

Table 4. Contact angle of electrospun nanofiber mats

Samples	Contact angle (°)					Ave. (°)
PVA/PU	52.0	49.5	54.5	53.5	50.5	52.0
PVA	44.0	42.5	42.5	43.5	40.5	42.6
PU	113.5	115.0	115.5	116.5	112.5	114.6

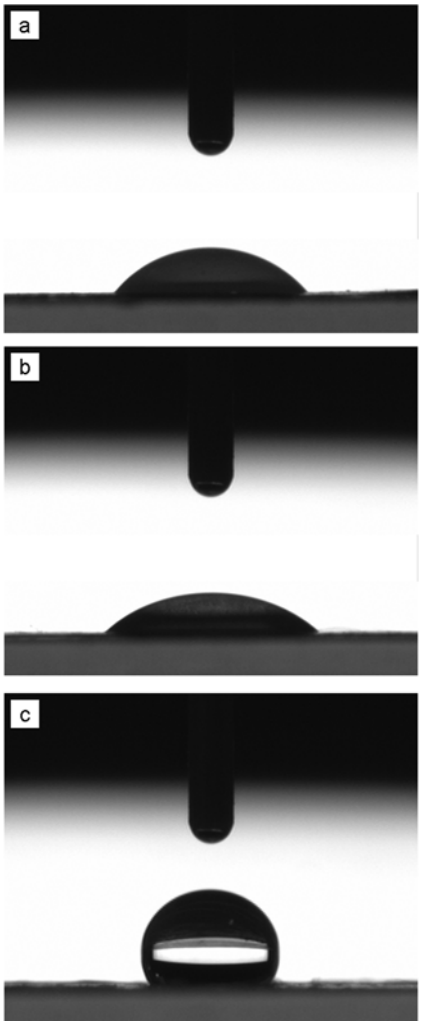

Figure 8. Water droplets resided on (a) PVA/PU blend nanofiber mat (52.0 °), (b) PVA nanofiber mat (42.5 °), and (c) PU nanofiber mat (115.0 °).

Table 5. Water absorption f electrospun nanofiber mats

Samples	Dried mat (g)	Water-absorbed mat (g)	Water absorption (%)
PVA/PU	0.50	2.28	78.07
PVA	0.50	3.36	85.12
PU	0.50	0.61	18.03

blend nanofiber mats. These values were averaged from five samples on different location of the mat, indicating that the PVA and PU nanofibers evenly distributed and formed the blend nanofiber mats with high porosity resulting into a hydrophilic surface.

The water absorption (in Table 5) of PVA nanofiber mats (85.12 %) was obviously much higher than that of PU nanofiber mats (18.03 %). And the water absorption of PVA/PU blend nanofiber mats remained a relatively high value (78.07 %). The main reason could be that the blend nanofiber mats exhibited higher surface-to-volume ratio and porosity. The results were consistent with those from contact angle tests.

Conclusion

In this study, the optimum conditions for PVA/PU blend nanofiber mats fabricated by dual-jet electrospinning were determined through the method of orthogonal experiment design. The main parameters affecting the fiber diameter was TCD, while the main parameters affecting the fiber diameter distribution was TTD. And the optimum electrospinning conditions were TCD of 20 cm, voltage of 18 kV and TTD of 4 cm in this system. The thermal analysis showed that the decomposition temperature of blend nanofiber mats was a little higher than that of pure PVA and PU nanofibers. Tensile tests showed the PVA/PU blend nanofiber mats were more flexible than pure PVA and stronger than pure PU. Contact angle (52.0 °) and water absorption (78.07 %) of PVA/PU blend nanofiber mats showed that the hydrophilicity of the PVA/PU blend nanofiber mats was very well. It was suggested that PVA/PU blend nanofiber mats had the possibility to be used as biomedical materials.

Acknowledgements

This work was financially supported by National Engineering Laboratory for Modern Silk and National Natural Science Foundation of China (Grant No.50903057).

References

1. J. Doshi and D. H. Reneker, *J. Electrostat.*, **35**, 151 (1995).
2. Z. M. Huang, Y. Z. Zhang, M. Kotaki, and S. Ramakrishna, *Compos. Sci. Technol.*, **63**, 2223 (2003).
3. L. M. Guerrini, M. P. D. Oliveira, M. C. Branciforti, T. A. Custódio, and R. E. S. Bretas, *J. Appl. Polym. Sci.*, **112**, 1680 (2009).
4. J. A. Ajao, A. Abiona, S. Chigome, J. B. Kana-Kana, and M. Maaza, *J. Mater. Sci.*, **45**, 713 (2010).
5. F. A. Sheikh, N. A. M. Barakat, M. A. Kanjwal, S. H. Jeon, H. S. Kang, and H. Y. Kim, *J. Appl. Polym. Sci.*, **115**, 3189 (2009).
6. J. Han, C. J. Branford-White, and L. M. Zhu, *Carbohyd. Polym.*, **79**, 214 (2010).
7. O. Suwantong, P. Opanasopit, U. Ruktanonchai, and P. Supaphol, *Polymer*, **48**, 7546 (2007).
8. J. A. Matthews, G. E. Wnek, D. G. Simpson, and G. L. Bowlin, *Biomacromolecules*, **3**, 232 (2002).
9. X. Y. Wang, C. Drew, S.-H. Lee, K. J. Senecal, J. Kumar, and L. A. Samuelson, *Nano. Lett.*, **2**, 1273 (2002).
10. P. P. Tsaia, H. S. Gibson, and P. Gibson, *J. Electrostat.*, **54**,

333 (2002).
11. B. Ding, H. Y. Kim, S. C. Lee, C. L. Shao, D. R. Lee, S. J. Park, G. B. Kwag, and K. J. Choi, *J. Polym. Sci. Pol. Phys.*, **40**, 1261 (2002).
12. M. Krumova, D. Lopez, R. Benavente, C. Mijangos, and J. M. Peresa, *Polymer*, **41**, 9265 (2000).
13. G. L. Ren, X. H. Xu, Q. Liu, J. Cheng, X. Y. Yuan, L. Wu, and Y. Wan, *React. Funct. Polym.*, **66**, 1559 (2006).
14. K. H. Hong, J. L. Park, I. H. Sul, J. H. Youk, and T. J. Kang, *J. Polym. Sci. Pol. Phys.*, **44**, 2468 (2006).
15. H. Homayoni, S. Abdolkarim, H. Ravandi, and M. Valizadeh, *J. Appl. Polym. Sci.*, **113**, 2507 (2009).
16. Y. T. Jia, J. Gong, X. H. Gu, H. Y. Kim, J. Dong, and X. Y. Shen, *Carbohyd. Polym.*, **67**, 403 (2007).
17. H. J. Wu, J. T. Fan, X. H. Qin, S. Mo, and J. O. Hinestroza, *J. Appl. Polym. Sci.*, **110**, 2525 (2008).
18. K. Bouchemal, S. Briançon, E. Perrier, H. Fessi, I. Bonnet, and N. Zydowicz, *Int. J. Pharm.*, **9**, 89 (2004).
19. H. T. Zhuo, J. L. Hu, S. J. Chen, and L. Yeung, *J. Appl. Polym. Sci.*, **109**, 406 (2008).
20. M. M. Demir, I. Yilor, E. Yilgor, and B. Erman, *Polymer*, **43**, 3303 (2002).
21. M. S. Khil, D. I. Cha, H. Y. Kim, I. S. Kim, and N. Bhattarai, *J. Appl. Biomaterials,* **67B**, 675 (2003).
22. H. T. Zhuo, J. L. Hu, and S. J. Chen, *Mater. Lett.*, **62**, 2074 (2008).
23. K. H. Lee, H. Y. Kim, Y. J. Ryu, K. W. Kim, and S. W. Choi, *J. Polym. Sci. Pol. Phys.*, **41**, 1256 (2003).
24. C. Y. Tang, P. P. Chen, and H. Q. Liu, *Polym. Eng. Sci.*, **48**, 1296 (2008).
25. X. J. Han, Z. M. Huang, C. L. He, L. Liu, and Q. S. Wu, *Polym. Compos.*, **29**, 579 (2008).
26. G. Taguchi, "System of Experimental Design: Engineering Methods to Optimize Quality and Minimize Costs", American Supplier Institute, New York, 1988.
27. C. H. Zhang, F. L. Yang, W. J. Wang, and B. Chen, *Sep. Purif. Technol.*, **61**, 276 (2008).
28. J. S. Lee, K. H. Choi, H. D. Ghim, S. S. Kim, D. H. Chun, H. Y. Kim, and W. S. Lyoo, *J. Appl. Polym. Sci.*, **93**, 1638 (2004).
29. K. Satoru, K. I. Keun, and M. Takehisa, *J. Biome. Mater. Res.*, **76**, 219 (2006).
30. P. Heikkilä and A. Harlin, *Eur. Polym. J.*, **44**, 3067 (2008).
31. T. Subbiah, G. S. Bhat, R. W. Tock, S. Parameswaran, and S. S. Ramkumar, *J. Appl. Polym. Sci.*, **96**, 557 (2005).
32. C. Wang, W. Zhang, Z. H. Huang, E. Y. Yan, and Y. H. Su, *Pigm. Resin. Technol.*, **35**, 278 (2006).
33. A. K. Haghi and M. Akbari, *Phys. Status. Solidi. A.*, **204**, 1830 (2007).
34. Y. Li, Z. M. Huang, and Y. D. Lu, *Eur. Polym. J.*, **42**, 1696 (2006).
35. S. L. Zhao, X. H. Wu, L. G. Wang, and Y. Huang, *J. Appl. Polym. Sci.*, **91**, 242 (2004).
36. G. S. Ryu, J. T. Oh, and H. Kim, *Fiber. Polym.*, **11**, 36 (2010).
37. C. S. Kong, T. H. Lee, K. H. Lee, and H. S. Kim, *J. Macromol. Sci. B*, **48**, 77 (2009).
38. S. M. Cakic, J. V. Stamenkovic, D. M. Djordjevic, and I. S. Ristic, *Polym. Degrad. Stabil.*, **94**, 2015 (2009).
39. F. Zhang, B. Q. Zuo, H. X. Zhang, and L. Bai, *Polymer*, **50**, 279 (2009).
40. M. Abdelaziz and E. M. Abdelrazek, *Physica B*, **390**, 1 (2007).
41. N. A. Peppas and P. J. Hansen, *J. Appl. Polym. Sci.*, **27**, 4787 (1982).
42. N. A. Peppas, *Makromol. Chem.*, **178**, 595 (1977).
43. R. M. Silverstein, F. X. Webster, and D. J. Klemie, "Spectrometric Identification of Organic Compounds", 7th ed., John Willey & Sons, New York, 2005.
44. B. H. Stuart, "Infrared Spectroscopy: Fundamental and Applications", John Wiley & Sons, New York, 2004.
45. G. A. Senich and W. J. MacKnight, *Macromolecules*, **13**, 106 (1980).
46. W. Zhang, Z. N. Zhang, and X. P. Wang, *J. Colloid. Interf. Sci.*, **333**, 346 (2009).